A DESIGN MODEL FOR STRAIN-SOFTENING AND STRAIN-HARDENING FIBER REINFORCED ELEMENTS FAILING IN BENDING – IMPLEMENTATION AND PARAMETRIC STUDIES

Mahsa Taheri, Joaquim A. O. Barros, Hamid R. Salehian

School of Engineering

Department of Civil Engineering

University do Minho

Azurém, 4800-085 Guimarães

TABLE OF CONTENTS

1 INTRODUCTION

Exhibiting remarkable compressive strength and durability, concrete is one of the most widely adopted materials for the construction of bridges. The tensile strength of concrete is contrarily low and is about 8 to 10 times less than its compressive strength. This inherent weak tensile strength of concrete makes it prone to the tensile cracking in tensile and flexural loadings and brings numerous problems in application of this material, mainly in its durability [1].

Reinforcement of cementitious materials with short randomly distributed fibers has been successfully practiced for more than 40 years [2]. In the Fiber Reinforced Cementitious (FRC) materials, reinforcing fibers allow crack bridging, a mechanism that improves the post-cracking residual strength of concrete with restraining crack opening [3]. Debonding and pulling out of fibers dissipate energy leading to a substantial increase in toughness, which enhances the energy absorption and ductility of the concrete composite [4,5].

2 MOMENT REDISTRIBUTION

Typical tensile stress–strain responses for plain and fiber reinforced concrete registered in experimental tensile tests are represented in Fig. 1. Curves obtained after different concrete ages are presented on the same diagram in order to show the behavior as a function of the cement hydration development. For plain concrete, the stress–strain diagram demonstrates a brittle behavior of the material. After peak stress, the residual strength decreases rapidly with increasing strain. When the macrocrack is localized, its propagation is very rapid and needs only low energy. In the fiber reinforced concrete, however, the stress decay in the post-peak of the stress-strain diagram is not so pronounced. In this case, due to the relatively large value of ultimate strain, the energy dissipation capacity is increased.
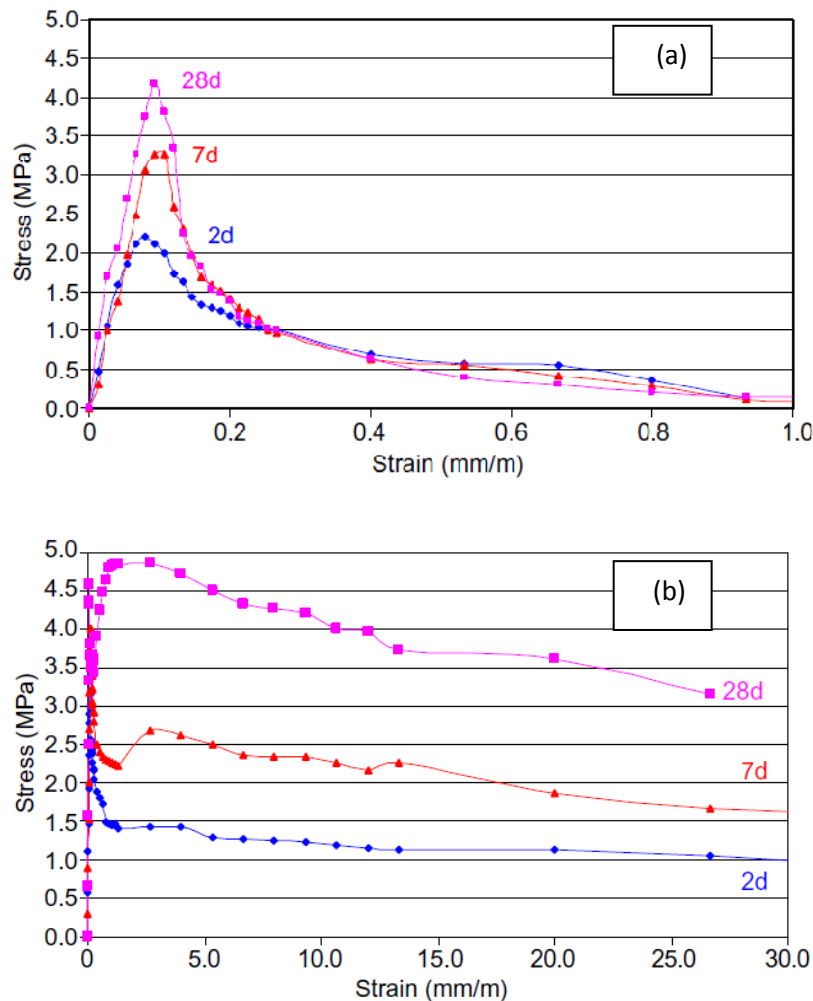
Fig. 1: Stress-strain relationship in direct tensile test; (a) for plain concrete; (b) for fiber reinforced concrete [3].

In the present report, the moment curvature relationship of FRC material is generated by utilizing the stress-strain (σ-ε) diagrams proposed by Soranakom and Mobasher, represented in Fig. 2 [6, 7].
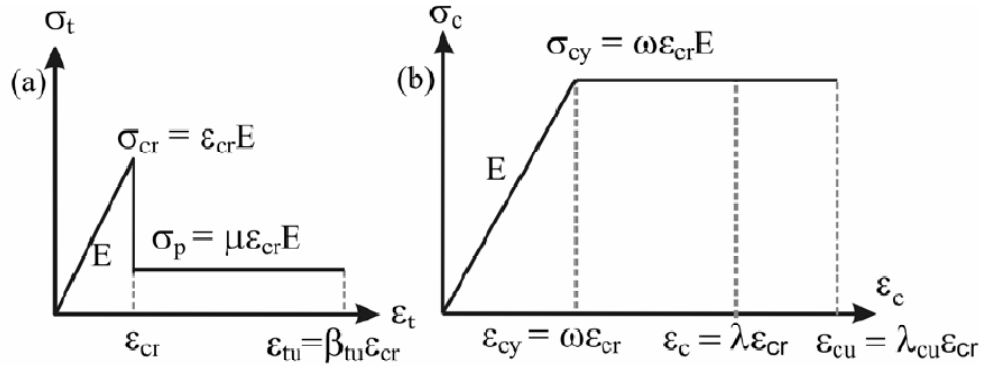

Fig. 2: Fiber reinforced concrete model; (a) Tension model; (b) Compression model [7]

These diagrams are based on an idealized model proposed by Lim et al. [8] for steel fiber concrete. The first model represents a bilinear response for tension and compression as shown in Fig. 2. According to the Fig. 2a, the tension response increases linearly from origin up to the cracking strain (ε_{cr}). After that, tensile stress remains constant at the post peak tensile strength (σ_p) that can be related to the ultimate tensile strength (σ_{cr}) by defining the normalized post-peak tensile strength (μ). This factor may be a function of fiber volume fraction, geometry, stiffness, and bond characteristics of the fibers, and also depends on the properties of the cement past surrounding the fibers [7]. The residual stress is assumed constant up to an ultimate strain (ε_{tu}).

Fig. 2b describes the compressive response with stress increasing linearly up to the yield point ($\sigma_{cy}, \varepsilon_{cy}$) and remains constant until termination point at the ultimate compressive strain (ε_{cu}). The elastic modulus in compression is assumed equal to tensile. In this model ω is the normalized compressive "yield" stress, and β_{tu} and λ_{cu} are normalized ultimate tensile and compressive strain, respectively. Both tension and compression models are expressed as [7]:

$$\sigma_t(\varepsilon_t) = \begin{cases} E\varepsilon_t & 0 \leq \varepsilon_t \leq \varepsilon_{cr} \\ \mu E\varepsilon_{cr} & \varepsilon_{cr} < \varepsilon_t \leq \varepsilon_{tu} \\ 0 & \varepsilon_t > \varepsilon_{tu} \end{cases} \tag{1}$$

$$\sigma_c(\varepsilon_c) = \begin{cases} E\varepsilon_c & 0 \leq \varepsilon_c \leq \varepsilon_{cy} \\ \omega E\varepsilon_{cr} & \varepsilon_{cy} \leq \varepsilon_c \leq \varepsilon_{cu} \\ 0 & \varepsilon_c > \varepsilon_{cu} \end{cases} \tag{2}$$

where σ_c, σ_t, ε_c and ε_t, are compressive and tensile stresses and strains, respectively. Soranakom and Mobasher [6] in their another model proposed a constitutive model for homogenized strain softening and hardening behavior of fiber reinforced concrete as shown in figure 3.
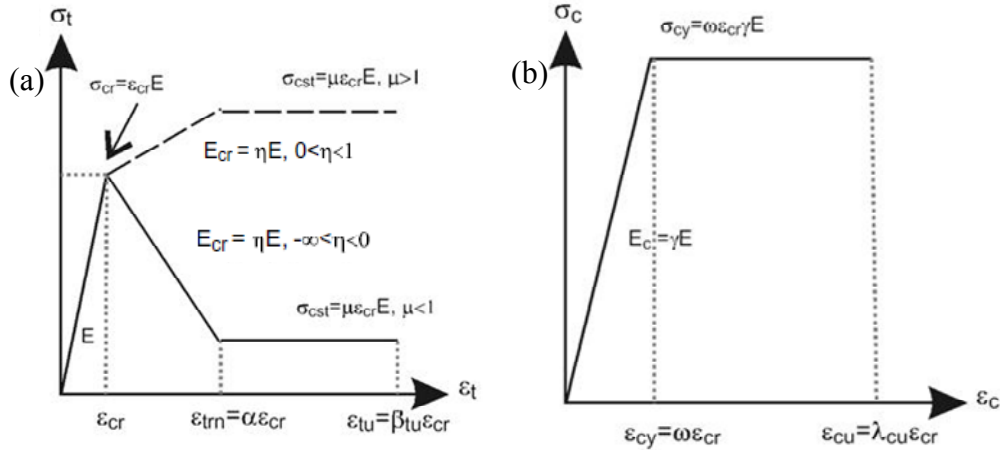

Fig. 3: Stress-strain diagrams for modeling the: a) compression and b) tensile behavior of fiber reinforced concrete with softening or hardening character [6].

As shown in Fig. 3b, the linear portion of an elastic–perfectly plastic compressive stress–strain response terminates at yield point (ε_{cy}, σ_{cy}) and remains constant at compressive "yield" stress σ_{cy} until the ultimate compressive strain ε_{cu}. Compressive modulus of materials (E_c) is defined as a ratio of tensile modulus (E) by representing the normalized compressive strain factor (γ). As shown in Fig. 3a, the tensile behavior is described by a trilinear diagram with an elastic range defined by tensile modulus (E), followed by a post-cracking modulus (E_{cr}) that can be obtained by using a post-crack modulus parameter (η). By setting η to either a negative or a positive value, the same model can be used to simulate strain softening or strain hardening materials, respectively. At the third region of tensile response, tensile stress remains in a constant stress value defined as σ_{cst}. For strain softening materials, σ_{cst} is equal to the post peak tensile strength represented by σ_p in previous model (Fig. 2a). The meaning of the others parameters of this model was already introduced. The stress–strain relationship for compression and tension can be expressed as [6]:

$$\sigma_t(\varepsilon_t) = \begin{cases} E\varepsilon_t & 0 \leq \varepsilon_t \leq \varepsilon_{cr} \\ E\varepsilon_{cr} + E_{cr}(\varepsilon_t - \varepsilon_{cr}) & \varepsilon_{cr} \leq \varepsilon_t \leq \varepsilon_{trn} \\ \mu E\varepsilon_{cr} & \varepsilon_{trn} \leq \varepsilon_t \leq \varepsilon_{tu} \\ 0 & \varepsilon_t > \varepsilon_{tu} \end{cases} \tag{3}$$

$$\sigma_c(\varepsilon_c) = \begin{cases} E_c\varepsilon_c & 0 \le \varepsilon_c \le \varepsilon_{cy} \\ E_c\varepsilon_{cy} & \varepsilon_{cy} \le \varepsilon_c \le \varepsilon_{cu} \\ 0 & \varepsilon_c > \varepsilon_{cu} \end{cases} \tag{4}$$

In the following equations, the model is represented in normalized form with utilizing the first cracking tensile strain (ε_{cr}) and tensile modulus (E) as two inherent parameters of the material [6]:

$$\frac{\sigma_t(\beta)}{E\varepsilon_{cr}} = \begin{cases} \beta & 0 \le \beta \le 1 \\ 1 + \eta(\beta - 1) & 1 \le \beta \le \alpha \\ \mu & \alpha \le \beta \le \beta_{tu} \\ 0 & \beta > \beta_{tu} \end{cases} \tag{5}$$

$$\frac{\sigma_c(\lambda)}{E\varepsilon_{cr}} = \begin{cases} \gamma\lambda & 0 \le \lambda \le \omega \\ \gamma\omega & \omega \le \lambda \le \lambda_{cu} \\ 0 & \lambda > \lambda_{cu} \end{cases} \tag{6}$$

where, the dimensionless parameters are represented from the following equations:

$$\omega = \frac{\varepsilon_{cy}}{\varepsilon_{cr}} \tag{7}$$

$$\alpha = \frac{\varepsilon_{trn}}{\varepsilon_{cr}} \tag{8}$$

$$\beta_{tu} = \frac{\varepsilon_{tu}}{\varepsilon_{cr}} \tag{9}$$

$$\lambda_{cu} = \frac{\varepsilon_{cu}}{\varepsilon_{cr}} \tag{10}$$

$$\gamma = \frac{E_c}{E} \tag{11}$$

$$\eta = \frac{E_{cr}}{E} \tag{12}$$

$$\mu = \frac{\sigma_{cst}}{E\varepsilon_{cr}} \tag{13}$$

The normalized tensile strain at the bottom fiber (β) and compressive strain at the top fiber (λ) are also defined as (Fig. 4):

$$\beta = \frac{\varepsilon_{tbot}}{\varepsilon_{cr}} \tag{14}$$

$$\lambda = \frac{\varepsilon_{ctop}}{\varepsilon_{cr}} \tag{15}$$

Due to linear variation of strain on the height of section, β and λ are linearly related together as the following equation:

$$\lambda = \frac{k}{1-k}\beta \tag{16}$$

where, k is the neutral axis depth ratio obtained by dividing the neutral axis depth by depth of section.

3 MOMENT-CURVATURE RESPONSE

When a bending moment is applied on a section of a beam, the curvature of section can be determined by dividing the top compressive strain by the depth of neutral axis. Representing relation between applied moment and established curvature for any stage of loading generates the moment-curvature diagram of the cross section. Representing the relation of moment-curvature of a cross section is a method for demonstrating strength, ductility, energy dissipation capacity, and the rigidity of the section under investigation. If a complete moment-curvature relationship is available, one can also observe strength reduction beyond the peak bending moment, as well as the influence of having a strain softening or strain hardening material [10].

However, the most fundamental requirement in predicting the moment curvature relationship of a flexural member is the knowledge of the behavior of its constituents in both tensile and compression loading.

4 CLOSE FORM SOLUTIONS FOR MOMENT-CURVATURE

By applying the Kirchhoff hypothesis, which assumes that a plane section remains plane after bending, and shear deformation of the section can be ignored, the moment curvature diagram for a rectangular cross section of a width b and a depth d, and composed of FRC materials, can be derived in accordance with the Fig. 4. The distribution of tensile and compressive stresses in this figure is in accordance with the model proposed by Soranakom and Mobasher [6]. The three possible stages of tensile strain at bottom fiber, $0 \leq \beta \leq 1$, $1 < \beta \leq \alpha$, and $\alpha < \beta \leq \beta_{tu}$, are represented in Fig. 4a, 4b, and 4c, respectively. Each of Stage 2 and 3 has two possible conditions due to the value of compressive strain at top fiber in either elastic ($0 < \lambda \leq \omega$) or plastic ($\omega < \lambda \leq \lambda_{cu}$) behavior in compression. Table 1 and 2, represent the normalized heights of compression and tension zones with respect to beam depth d and the normalized magnitudes of stress at the vertices with respect to the first cracking stress ($E\varepsilon_{cr}$), respectively. The deduction of the expressions in Tables 1 and 2 can be found elsewhere [9].
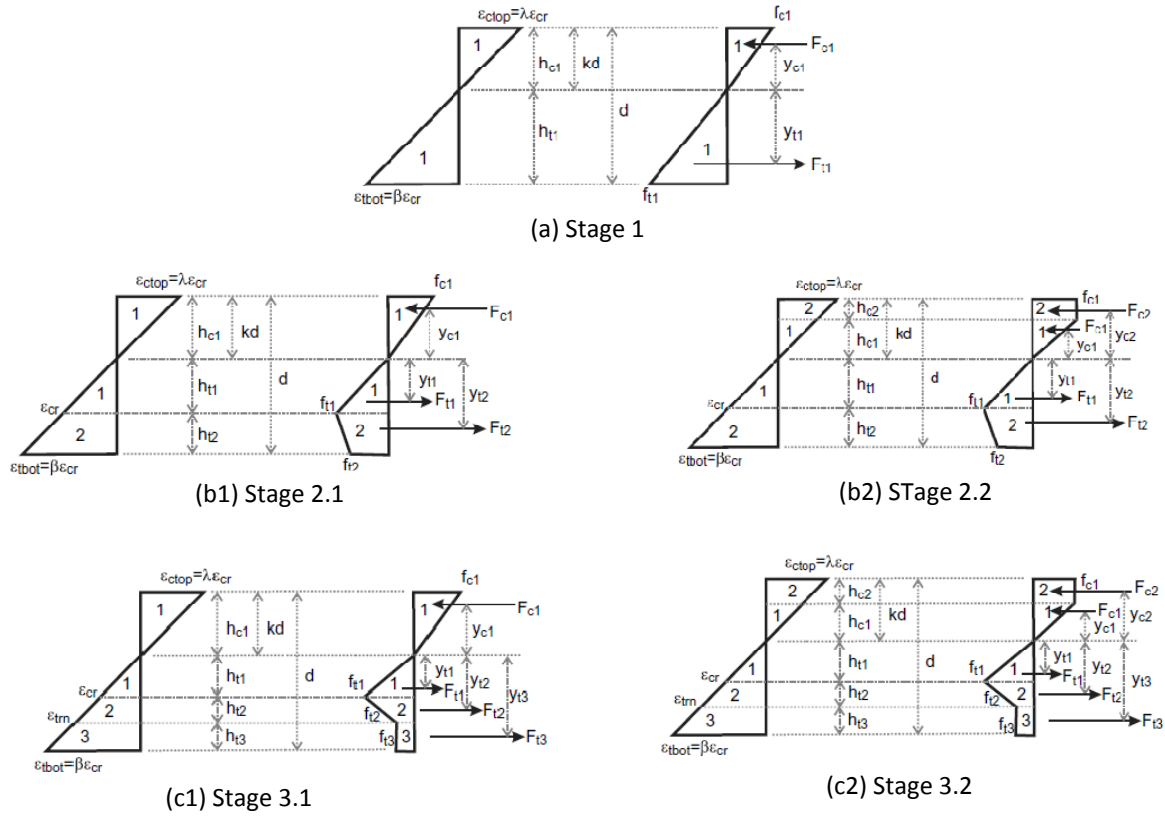
(a) Stage 1

(b1) Stage 2.1

(b2) STage 2.2

(c1) Stage 3.1

(c2) Stage 3.2

Fig. 4: Stress-strain diagram at different stages of normalized tensile strain at the bottom fiber (β): (a) $0 \leq \beta \leq 1$ and $0 < \lambda \leq \omega$; (b.1) $1 < \beta \leq \alpha$ and $0 < \lambda \leq \omega$; (b.2) $1 < \beta \leq \alpha$ and $\omega < \lambda \leq \lambda_{cu}$; (c.1) $\alpha < \beta \leq \beta_{tu}$ and $0 < \lambda \leq \omega$; (c.2) $\alpha < \beta \leq \beta_{tu}$ and $\omega < \lambda \leq \lambda_{cu}$ [6].

Table 1: Normalized height of compression and tension zones for each stage of normalized tensile strain at bottom fiber (β) [6, 9].

Normalized stress	Stage 1 $0 \leq \beta \leq 1$ $0 \leq \lambda \leq \omega$	Stage 2.1 $1 \leq \beta \leq \alpha$ $0 \leq \lambda \leq \omega$	Stage 2.2 $1 \leq \beta \leq \alpha$ $\omega < \lambda \leq \lambda_{cu}$	Stage 3.1 $\beta > \alpha$ $0 \leq \lambda \leq \omega$	Stage 3.2 $\beta > \alpha$ $\omega < \lambda \leq \lambda_{cu}$
$\dfrac{h_{c2}}{d}$	–	–	$\dfrac{k\beta - \omega(1-k)}{\beta}$	–	$\dfrac{k\beta - \omega(1-k)}{\beta}$
$\dfrac{h_{c1}}{d}$	k	k	$\dfrac{\omega(1-k)}{\beta}$	k	$\dfrac{\omega(1-k)}{\beta}$
$\dfrac{h_{t1}}{d}$	1-k	$\dfrac{1-k}{\beta}$	$\dfrac{1-k}{\beta}$	$\dfrac{1-k}{\beta}$	$\dfrac{1-k}{\beta}$
$\dfrac{h_{t2}}{d}$	–	$\dfrac{(1-k)(\beta-1)}{\beta}$	$\dfrac{(1-k)(\beta-1)}{\beta}$	$\dfrac{(1-k)(\alpha-1)}{\beta}$	$\dfrac{(1-k)(\alpha-1)}{\beta}$
$\dfrac{h_{t3}}{d}$	–	–	–	$\dfrac{(1-k)(\beta-\alpha)}{\beta}$	$\dfrac{(1-k)(\beta-\alpha)}{\beta}$

Table 2: Normalized stress at vertices in the stress diagram for each stage of normalized tensile strain at bottom fiber (β) [6, 9].

Normalized stress	Stage 1 $0 \leq \beta \leq 1$ $0 \leq \lambda \leq \omega$	Stage 2.1 $1 \leq \beta \leq \alpha$ $0 \leq \lambda \leq \omega$	Stage 2.2 $1 \leq \beta \leq \alpha$ $\omega < \lambda \leq \lambda_{cu}$	Stage 3.1 $\beta > \alpha$ $0 \leq \lambda \leq \omega$	Stage 3.2 $\beta > \alpha$ $\omega < \lambda \leq \lambda_{cu}$
$\dfrac{f_{c2}}{E\varepsilon_{cr}}$	–	–	$\omega\gamma$	–	$\omega\gamma$s
$\dfrac{f_{c1}}{E\varepsilon_{cr}}$	$\dfrac{\gamma\beta k}{1-k}$	$\dfrac{\gamma\beta k}{1-k}$	$\omega\gamma$	$\dfrac{\gamma\beta k}{1-k}$	$\omega\gamma$
$\dfrac{f_{t1}}{E\varepsilon_{cr}}$	β	1	1	1	1
$\dfrac{f_{t2}}{E\varepsilon_{cr}}$	–	$1 + \eta\,(\beta - 1)$	$1 + \eta\,(\beta - 1)$	$1 + \eta\,(\alpha - 1)$	$1 + \eta\,(\alpha - 1)$
$\dfrac{f_{t3}}{E\varepsilon_{cr}}$	–	–	–	μ	μ

The force components and their lines of action shown in Fig. 4 are obtained from the area and centroid of stress in each zone. The normalized values with respect to cracking tensile force ($bdE\varepsilon_{cr}$) and beam depth d are presented in Tables 3 and 4, respectively. The deduction of the expressions in Tables 1 and 2 can be found elsewhere [9].

At each stage of applied tensile strain, β, the net force is obtained as the difference between the tensile and compression forces calculated from Table 3, equated to zero for internal equilibrium in accordance with the fourth column of Table 5, and solved for the neutral axis depth ratio k. It is notable that the expressions for net force in Stage 2.1 and 3 are in the quadratic forms and result in two acceptable solutions for k. With a large scale of numerical tests covering a practical range of material parameters, only one solution of k yields the valid value in the range $0 < k < 1$ [6]. These values are presented in Table 6. After achieving the correct value of k in each stage, internal moment is obtained by operating on the force components and their distance from neutral axis as the equations represented in the fifth column of the Table 5. Related curvature also is determined as the ratio of compressive strain at top fiber to the depth of neutral axis.

Table 3: Normalized force component for each stage of normalized tensile strain at bottom fiber (β) [6, 9]

Normalized stress	Stage 1 $0 \leq \beta \leq 1$ $0 \leq \lambda \leq \omega$	Stage 2.1 $1 \leq \beta \leq \alpha$ $0 \leq \lambda \leq \omega$	Stage 2.2 $1 \leq \beta \leq \alpha$ $\omega < \lambda \leq \lambda_{cu}$	Stage 3.1 $\beta > \alpha$ $0 \leq \lambda \leq \omega$	Stage 3.2 $\beta > \alpha$ $\omega < \lambda \leq \lambda_{cu}$
$\dfrac{F_{c2}}{bdE\varepsilon_{cr}}$	$-$	$-$	$\dfrac{\omega\gamma}{\beta}(\beta k + \omega k - \omega)$	$-$	$\dfrac{\omega\gamma}{\beta}(\beta k + \omega k - \omega)$
$\dfrac{F_{c1}}{bdE\varepsilon_{cr}}$	$\dfrac{\beta\gamma k^2}{2(1-k)}$	$\dfrac{\beta\gamma k^2}{2(1-k)}$	$\dfrac{\omega^2\gamma}{2\beta}(1-k)$	$\dfrac{\beta\gamma k^2}{2(1-k)}$	$\dfrac{\omega^2\gamma}{2\beta}(1-k)$
$\dfrac{F_{t1}}{bdE\varepsilon_{cr}}$	$\dfrac{\beta}{2}(1\text{-}k)$	$\dfrac{(1-k)}{2\beta}$	$\dfrac{(1-k)}{2\beta}$	$\dfrac{(1-k)}{2\beta}$	$\dfrac{(1-k)}{2\beta}$
$\dfrac{F_{t2}}{bdE\varepsilon_{cr}}$	$-$	$\dfrac{(1-k)(\beta-1)(\eta\beta-\eta+2)}{2\beta}$	$\dfrac{(1-k)(\beta-1)(\eta\beta-\eta+2)}{2\beta}$	$\dfrac{(1-k)(\alpha-1)(\eta\alpha-\eta+2)}{2\beta}$	$\dfrac{(1-k)(\alpha-1)(\eta\alpha-\eta+2)}{2\beta}$
$\dfrac{F_{t3}}{bdE\varepsilon_{cr}}$	$-$	$-$	$-$	$\dfrac{(1-k)(\beta-\alpha)\mu}{\beta}$	$\dfrac{(1-k)(\beta-\alpha)\mu}{\beta}$

Table 4: Normalized moment arm of force component for each stage of normalized tensile strain at bottom fiber (β) [6, 9]

Normalized stress	Stage 1 $0 \leq \beta \leq 1$ $0 \leq \lambda \leq \omega$	Stage 2.1 $1 \leq \beta \leq \alpha$ $0 \leq \lambda \leq \omega$	Stage 2.2 $1 \leq \beta \leq \alpha$ $\omega < \lambda \leq \lambda_{cu}$	Stage 3.1 $\beta > \alpha$ $0 \leq \lambda \leq \omega$	Stage 3.2 $\beta > \alpha$ $\omega < \lambda \leq \lambda_{cu}$
$\dfrac{y_{c2}}{d}$	—	—	$\dfrac{k\beta + \omega(1-k)}{2\beta}$	—	$\dfrac{k\beta + \omega(1-k)}{2\beta}$
$\dfrac{y_{c1}}{d}$	$\dfrac{2}{3}k$	$\dfrac{2}{3}k$	$\dfrac{2}{3}\dfrac{\omega(1-k)}{\beta}$	$\dfrac{2}{3}k$	$\dfrac{2}{3}\dfrac{\omega(1-k)}{\beta}$
$\dfrac{y_{t1}}{d}$	$\dfrac{2}{3}(1-k)$	$\dfrac{2}{3}\dfrac{(1-k)}{\beta}$	$\dfrac{2}{3}\dfrac{(1-k)}{\beta}$	$\dfrac{2}{3}\dfrac{(1-k)}{\beta}$	$\dfrac{2}{3}\dfrac{(1-k)}{\beta}$
$\dfrac{y_{t2}}{d}$	—	$\dfrac{2\eta\beta^2 - \eta\beta - \eta + 3\beta + 3}{3\beta(\eta\beta - \eta + 2)}(1-k)$	$\dfrac{2\eta\beta^2 - \eta\beta - \eta + 3\beta + 3}{3\beta(\eta\beta - \eta + 2)}(1-k)$	$\dfrac{2\eta\alpha^2 - \eta\alpha - \eta + 3\alpha + 3}{3\beta(\eta\alpha - \eta + 2)}$	$\dfrac{2\eta\alpha^2 - \eta\alpha - \eta + 3\alpha + 3}{3\beta(\eta\alpha - \eta + 2)}$
$\dfrac{y_{t3}}{d}$	—	—	—	$\dfrac{(\alpha + \beta)}{2\beta}(1-k)$	$\dfrac{(\alpha + \beta)}{2\beta}(1-k)$

Table 5: Equilibrium of force, moment and curvature for each stage of normalized tensile strain at bottom fiber (β) [6].

Stage	Tension	Compression	Force equilibrium	Internal moment
1	$0 \leq \beta \leq 1$	$0 \leq \lambda \leq \omega$	$-F_{c1} + F_{t1}$	$F_{c1}y_{c1} + F_{t1}y_{t1}$
2.1	$1 < \beta \leq \alpha$	$0 \leq \lambda \leq \omega$	$-F_{c1} + F_{t1} + F_{t2}$	$F_{c1}y_{c1} + F_{t1}y_{t1} + F_{t2}y_{t2}$
2.2	$1 < \beta \leq \alpha$	$\omega < \lambda \leq \lambda_{cu}$	$-F_{c1} - F_{c2} + F_{t1} + F_{t2}$	$F_{c1}y_{c1} + F_{c2}y_{c2} + F_{t1}y_{t1} + F_{t2}y_{t2}$
3.1	$\beta > \alpha$	$0 \leq \lambda \leq \omega$	$-F_{c1} + F_{t1} + F_{t2} + F_{t3}$	$F_{c1}y_{c1} + F_{t1}y_{t1} + F_{t2}y_{t2} + F_{t3}y_{t3}$
3.2	$\beta > \alpha$	$\omega < \lambda \leq \lambda_{cu}$	$-F_{c1} - F_{c2} + F_{t1} + F_{t2} + F_{t3}$	$F_{c1}y_{c1} + F_{c2}y_{c2} + F_{t1}y_{t1} + F_{t2}y_{t2} + F_{t3}y_{t3}$

At stag i of loading, the moment and curvature (M_i , ϕ_i), are obtained from the following equation:

$$M_i = M_i' M_{cr} \tag{17}$$

$$\phi_i = \phi_i' \phi_{cr} \tag{18}$$

where, M_i' and ϕ_i' are normalized moment and curvature at stage i obtained from Table 6. M_{cr} and ϕ_{cr} are also cracking moment and curvature calculated for a rectangular section from the following equations:

$$M_{cr} = \frac{1}{6} bd^2 (E\varepsilon_{cr}) \tag{19}$$

$$\phi_{cr} = \frac{2\varepsilon_{cr}}{d} \tag{20}$$

Table 6: Neutral axis depth ratio, normalized moment and curvature for each stage of normalized tensile [6, 9].

Stage	K	M'	ϕ'
1	$k_1 = \begin{cases} \dfrac{1}{2} & for\ \gamma = 1 \\[2mm] \dfrac{-1+\sqrt{\gamma}}{-1+\gamma} & for\ \gamma < 1\ or\ \gamma > 1 \end{cases}$	$M'_1 = \dfrac{2\beta[(\gamma-1)K_1^3 + 3K_1^2 - 3K_1 + 1]}{1 - K_1}$	$\phi'_1 = \dfrac{\beta}{2(1 - K_1)}$
2.1	$k_{21} = \dfrac{\beta^2\gamma + D_{21} - \sqrt{\gamma^2\beta^4 + D_{21}\gamma\beta^2}}{D_{21}}$ $D_{21} = \eta(\beta^2 - 2\beta + 1) + 2\beta - \beta^2\gamma - 1$	$M'_{21} = \dfrac{(2\beta\gamma + C_{21})K_{21}^3 - 3C_{21}K_{21}^2 + 3C_{21}K_{21} - C_{21}}{1 - K_{21}}$ $C_{21} = \dfrac{-2\eta\beta^3 + 3\eta\beta^2 - 3\beta^2 - \eta + 1}{\beta^2}$	$\phi'_{21} = \dfrac{\beta}{2(1 - K_{21})}$
2.2	$K_{22} = \dfrac{D_{22}}{D_{22} + 2\omega\gamma\beta}$ $D_{22} = \eta(\beta^2 - 2\beta + 1) + 2\beta + \omega^2\gamma - 1$	$M'_{22} = (3\omega\gamma + C_{22})K_{22}^2 - 2C_{22}K_{22} + C_{22}$ $C_{22} = \dfrac{2\eta\beta^3 - 3\eta\beta^2 + 3\beta^2 - \omega^3\gamma + \eta - 1}{\beta^2}$	$\phi\_22^{´´} = \dfrac{\beta}{2(1 - K_{22})}$
3.1	$K_{31} = \dfrac{D_{31} - \sqrt{\gamma\beta^2 D_{31}}}{D_{31} - \beta^2\gamma}$ $D_{31} = \eta(\alpha^2 - 2\alpha + 1) + 2\mu(\beta - \alpha) + 2\alpha - 1$	$M'_{31} = \dfrac{(C_{31} - 2\beta\gamma)K_{31}^3 - 3C_{31}K_{31}^2 + 3C_{31}K_{31} - C_{31}}{K_{31} - 1}$ $C_{31} = \dfrac{3(\mu\beta^2 - \mu\alpha^2 - \eta\alpha^2 + \alpha^2) + 2\eta\alpha^3 + \eta - 1}{\beta^2}$	$\phi'_{31} = \dfrac{\beta}{2(1 - K_{31})}$
3.2	$K\_32 = D\_32/(D\_32 + 2\omega\gamma\beta)$ $D_{32} = \omega^2\gamma + \eta\alpha^2 + 2(\mu\beta - \eta\alpha - \mu\alpha + \alpha) + \eta - 1$	$M'_{32} = (C_{32} + 3\omega\gamma)K_{32}^2 - 2C_{32}K_{32} + C_{32}$ $C_{32} = \dfrac{3(\mu\beta^2 - \mu\alpha^2 - \eta\alpha^2 + \alpha^2) + 2\eta\alpha^3 - \omega^3\gamma + \eta - 1}{\beta^2}$	$\phi'_{32} = \dfrac{\beta}{2(1 - K_{32})}$

5 ALGORITHM TO PREDICT MOMENT-CURVATURE RESPONSE OF FRC MATERIALS

To generate computer software for calculating moment-curvature response of bending members made from fiber reinforced concrete, an algorithm is illustrated based on Soranakom and Mobasher model proposed for behavior of FRC in tensile and compression. Inherent mechanical properties of material obtained according to the conventional standard tests and used with geometrical details of section to achieve parameters $\omega, \alpha, \beta_{tu}, \lambda_{cu}, \gamma, \eta$, and μ by using Eq. 7-13, respectively. The procedure used for obtaining the complete moment-curvature relationship for a rectangular cross section is given bellow:

The normalized ultimate tensile strain (β_{tu}) is divided in discrete values obtained from the following equation:

$$\Delta\beta = \frac{\beta_{tu}}{A} \tag{21}$$

where, A is accuracy index of calculation and can be represented by operator at the beginning of calculation.

The normalized tensile strain at bottom fiber (β) is increased uniformly from $\Delta\beta$ to β_{tu}.

For selected value of β, parameter k is calculated by trial and error. At each loading stage, according to the value of β, the stage of loading is detected and base on it, one of the expressions given in Table 6 for stages 1, 2.1, 2.2, 3.1, or 3.2 is utilized periodically to obtain k. According to the value obtained for k, the net force of section obtained as the difference between the tensile and compression forces is calculated from Table 3. If the net force was little or equal than a constant value represented as acceptable tolerance, the correct value of k is obtained. Otherwise parameter k is calculated by using the next expression. At the end of this step, the stage of load bearing of section is also represented.

After achieving the correct value neutral axis depth ratio (k) and the stage of loading, normalized moment (M_i') and curvature (ϕ_i') are obtained from expressions given in Table 6.

Moment and curvature of each stage are obtained from Eq. 17 and 18, respectively. The value of cracking moment and curvature in these equations can be calculated in accordance with the material properties that are represented by user in primary step of calculation.

Steps 3-5 are repeated to calculate another point of moment-curvature diagram.

Algorithm is terminated when normalized tensile strain at bottom fiber achieves it ultimate value and the ultimate tensile strain is governed.

Azurém – 4800-058 Guimarães

6 MODEL APPRAISAL

To evaluate the accuracy of proposed algorithm mentioned earlier, the results of the software developed according to the algorithm were compared to the results obtained from the DOCROS software. According to the model implemented in DOCROS, a cross section is discretized in layers that can have distinct constitutive laws for the characterization of the behavior of the material that constitute these layers. A cross section can be composed of plain concrete and FRC layers, and can include steel bars and fiber reinforced polymer reinforcing elements. The cross section can be subjected to axial load and increase bending curvature. The position of the neutral axis is determined from the equilibrium of the axial force. Detailed description can be found [11]. This appraisal was done for a beam made with fiber reinforced concrete failing in bending. The cross section has a width of 300 mm and a depth of 400 mm. The stress-strain relationship adopted to simulate the compression behavior of the FRP is represented in Fig. 5, while the two stress-strain diagrams depicted in Fig. 6 were considered for modeling its tensile behavior, one assuming that the FRC presents a strain-softening response, and the other considering this composite has a strain-stiffening behavior.
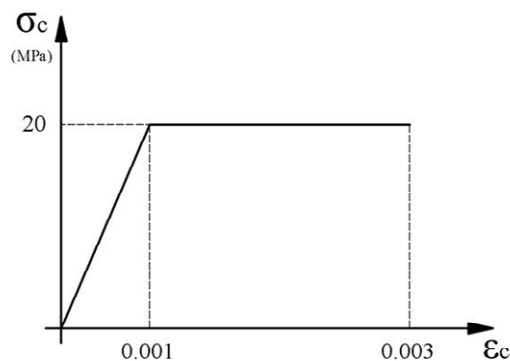

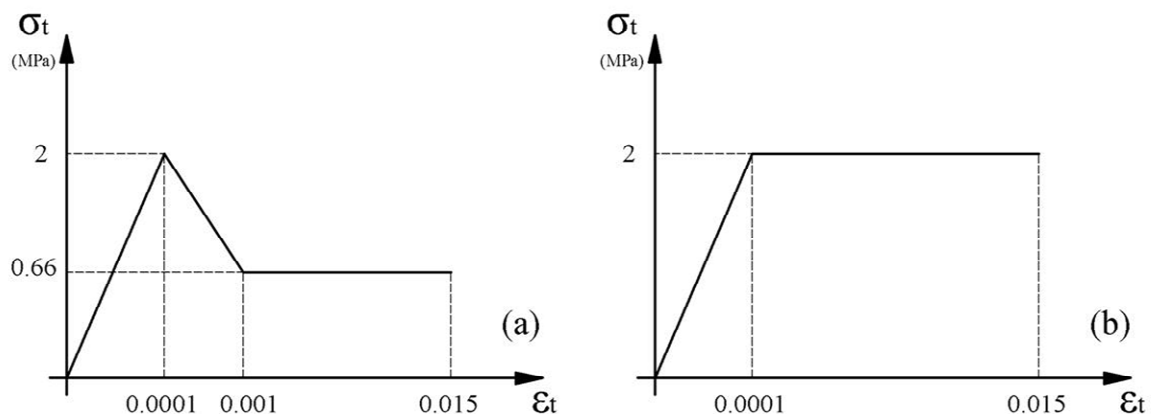Fig. 5: Compression response of FRC material

Fig. 6: Tensile modeling of FRC material; (a) strain softening, (b) strain hardening

Tensile behavior of FRC material is assumed in both strain softening and strain hardening as shown in Fig. 6a and 6b, respectively.

behavior of FRC material is assumed in both strain softening and strain hardening as shown in Fig. 6a and 6b, respectively.
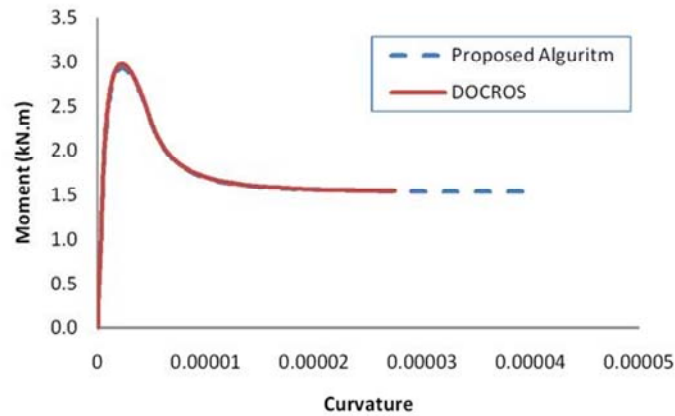

Fig. 7: Moment-curvature response of strain softening behavior of FRC
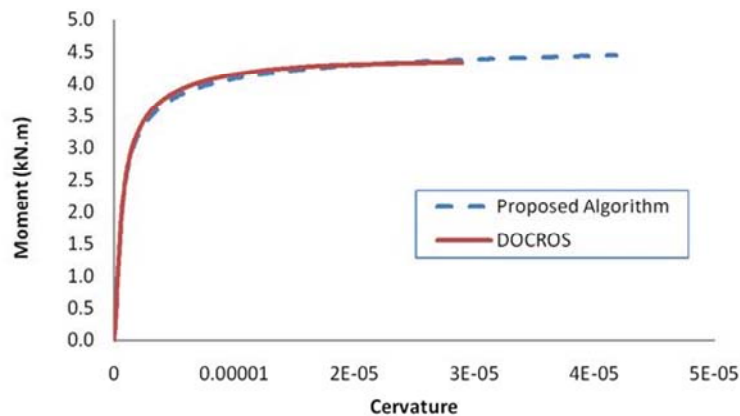

Fig. 8: Moment-curvature response of strain hardening behavior of FRC

The moment-curvature relationships obtained from proposed algorithm and DOCROS software are compared in the Fig. 7 and 8 for strain softening and strain hardening behavior of FRC, respectively. According to the Fig. 7 and 8, the results of proposed algorithm has a good agreement with those obtained from DOCROS software in both strain softening and strain hardening behavior of FRC. As shown Fig. 7, the moment-curvature relationship of a FRC material with strain softening has a sharply drop, right after achieving the resisting moment of section that is calculated 29 kN.m for studied beam section. This value is about 1.8 time greater than the cracking moment of the section. However in the case of strain hardening behavior, the moment-curvature relationship continues to increase up to the

18/35

ultimate point. Moment capacity obtained in this kind of behavior is higher than the last one, and is calculated 45 kN.m for the case of studied beam section. This value is about 2.8 time greater then the cracking moment of the section.

7 PARAMETRIC STUDIES OF MATERIAL PARAMETERS

Two sets of parametric studies were investigated to show the behavior of strain softening and strain hardening materials and their effects on moment-curvature response. Figures 9 to 11 present the parametric study of a typical strain softening material that some parameters were specified as a compressive to tensile strength ratio $\gamma\omega = 10$, normalized ultimate compressive strain $\lambda_{cu} = 30$ and ultimate tensile strain $\beta_{tu} = 150$. For each case of study, all parameters were held constant to the typical values while the parameters subjected to study were varied. It is noticeable that parameters α, μ and η are related together by Eq. 22:

$$\eta = -\frac{(1-\mu)}{(\alpha-1)} \tag{22}$$

Fig. 9a and 9b depicts the compressive and tension model with the transition strain α varied from 1.01 to 15. Fig. 9c indicates when α increases the moment-curvature response increases too.
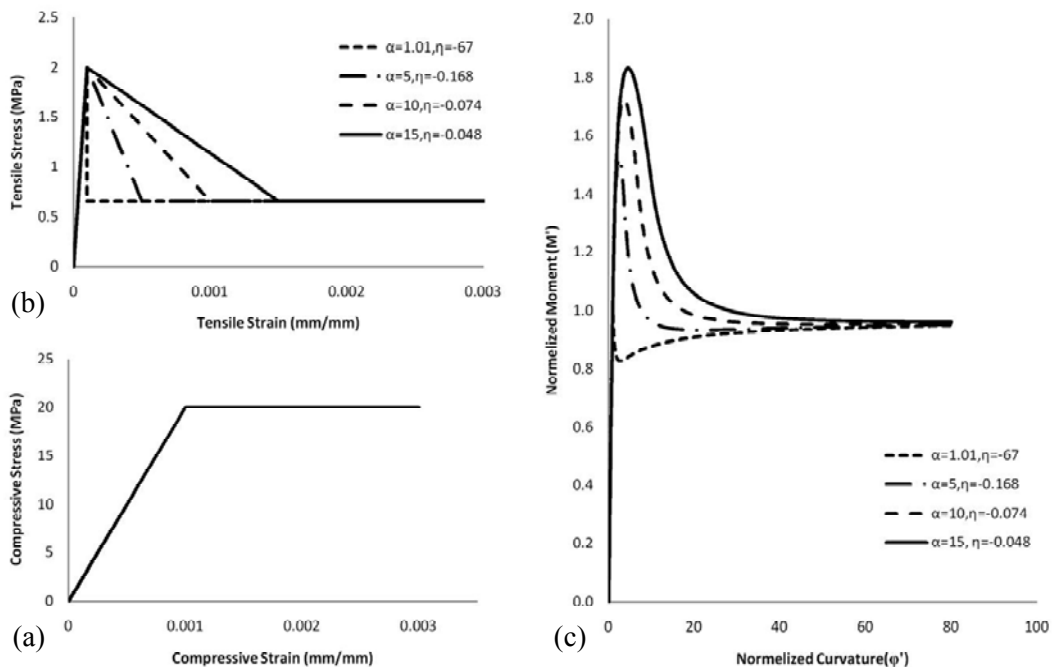

Fig. 9: Parametric study of typical strain softening material: the effect of parameter α for $E = 20\,GPa, \varepsilon_{cr} = 0.0001, \mu = 0.33, \beta_{tu} = 150, \gamma = 1, \omega = 10, \lambda_{cu} = 30$; (a) compressive stress-strain relationship, (b) tensile stress-strain relationship, (c) moment-curvature diagram.
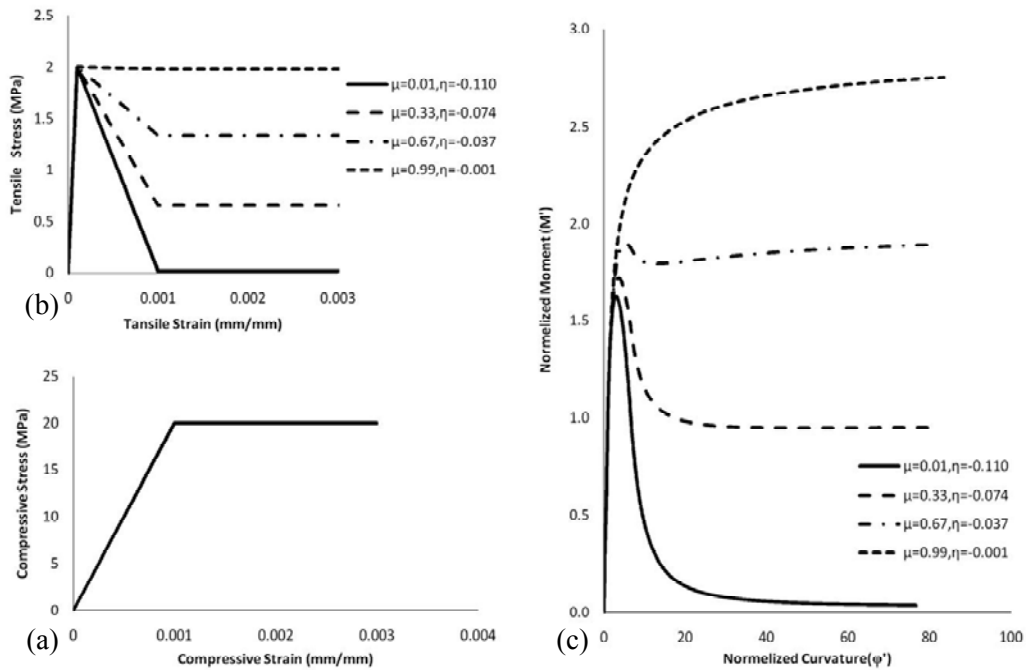
Fig. 10: Parametric study of typical strain softening material: the effect of parameter μ for $E = 20\,GPa, \varepsilon_{cr} = 0.0001, \alpha = 10, \beta_{tu} = 150, \gamma = 1, \omega = 10, \lambda_{cu} = 30$; (a) compressive stress-strain relationship, (b) tensile stress-strain relationship, (c) moment-curvature diagram.
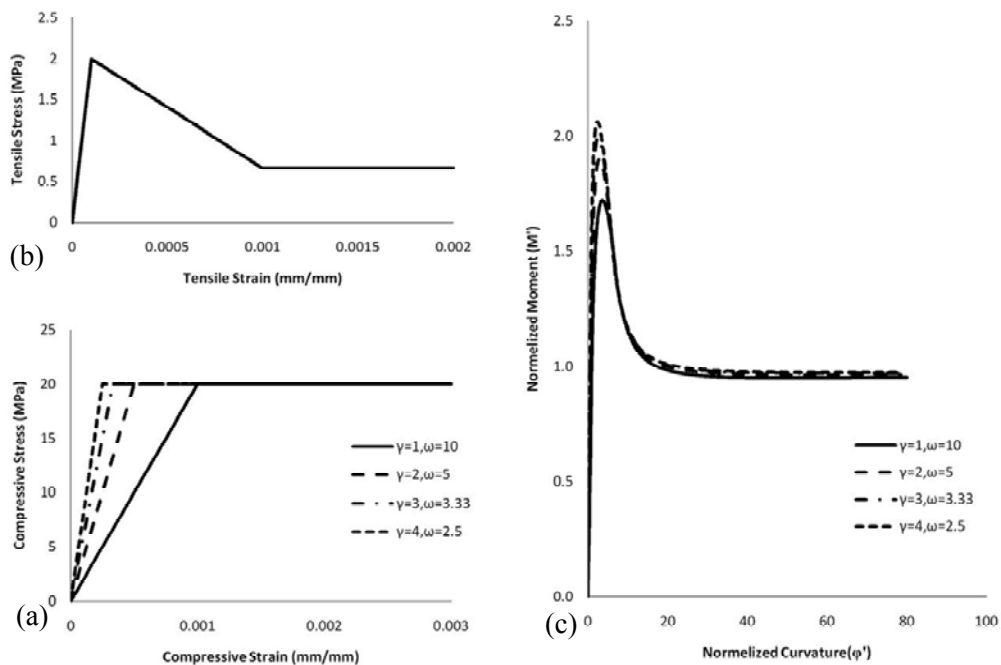

Fig. 11: Parametric study of typical strain softening material: the effect of parameter γ for $E = 20\,GPa, \varepsilon_{cr} = 0.0001, \alpha = 10, \beta_{tu} = 150, \mu = 0.33, \lambda_{cu} = 30$; (a) compressive stress-strain relationship, (b) tensile stress-strain relationship, (c) moment-curvature diagram.

(b)

Figs. 10a and 10b depicts that μ varied from 0.01 to 0.99 and Fig. 10c shows that moment-curvature response is very sensitive to the variations in parameter μ. The flexural response changes from a brittle to ductile character as μ changes from 0.01 to 0.99.

Figs. 11a and 11b investigate the effects of the increase in relative compressive to tensile stiffness from $0.1 < \frac{\gamma}{\omega} < 1.6$ at a fixed compressive to tensile strength ratio $\gamma\omega = 10$. Fig. 11c shows that the changes in the relative stiffness slightly affect on moment-curvature response. Figures 12 to 14 present the parametric study of a typical strain hardening material, with a compressive to tensile cracking strength ratio of $\gamma\omega = 10$, normalized ultimate compressive strain $\lambda_{cu} = 30$ and ultimate tensile strain $\beta_{tu} = 150$. The parameters α, μ and η are related together by Eq. 23.

$$\eta = \frac{(\mu-1)}{(\alpha-1)} \tag{23}$$

Fig. 12a and 12b shows the compression and tension model of a typical tensile strain hardening material with varying α from 1.01 to 15. Fig. 12c shows that when α increases directly increases the moment-curvature response. Fig. 13a and 13b indicate that when the parameter η varies from 0.01 to 0.99, a significant increase of the momen-curvature diagram occur.
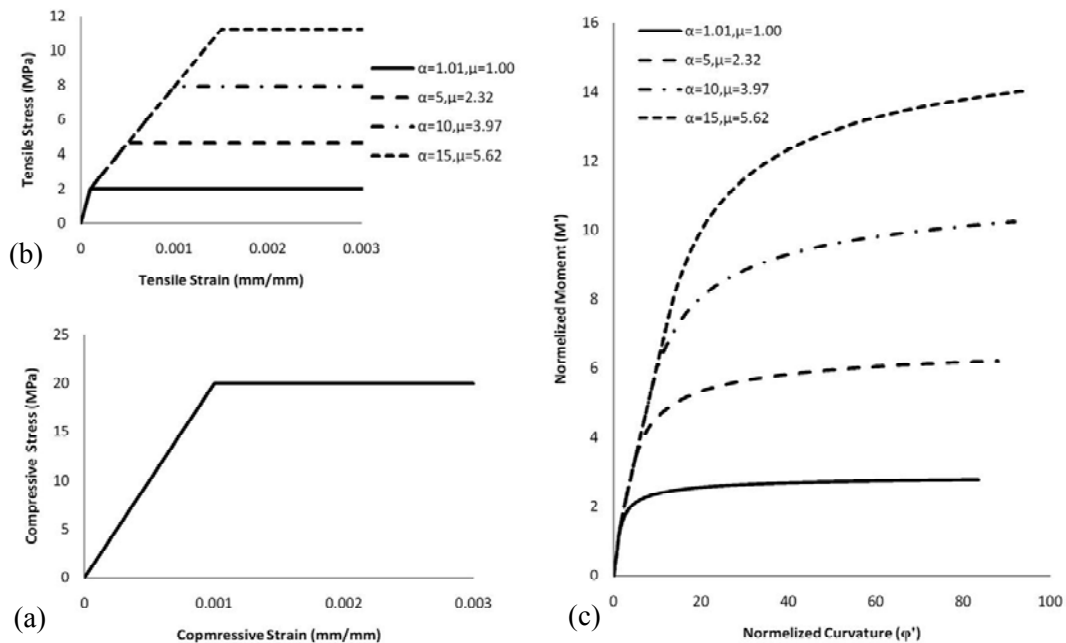

Fig. 12: Parametric study of typical strain hardening material: the effect of parameter α for $E = 20\ GPa, \varepsilon_{cr} = 0.0001, \eta = 0.33, \gamma = 1, \omega = 10, \beta_{tu} = 150,\ \lambda_{cu} = 30$; (a) compresive stress-strain relationship, (b) tensile stress-strain relationship, (c) moment-curvature diagram.

Fig. 13: Parametric study of typical strain hardening material: the effect of parameter η for $E = 20\ GPa, \varepsilon_{cr} = 0.0001, \alpha = 10, \gamma = 1, \omega = 10, \beta_{tu} = 150,\ \lambda_{cu} = 30$; (a) compresive stress-strain relationship, (b) tensile stress-strain relationship, (c) moment-curvature diagram.
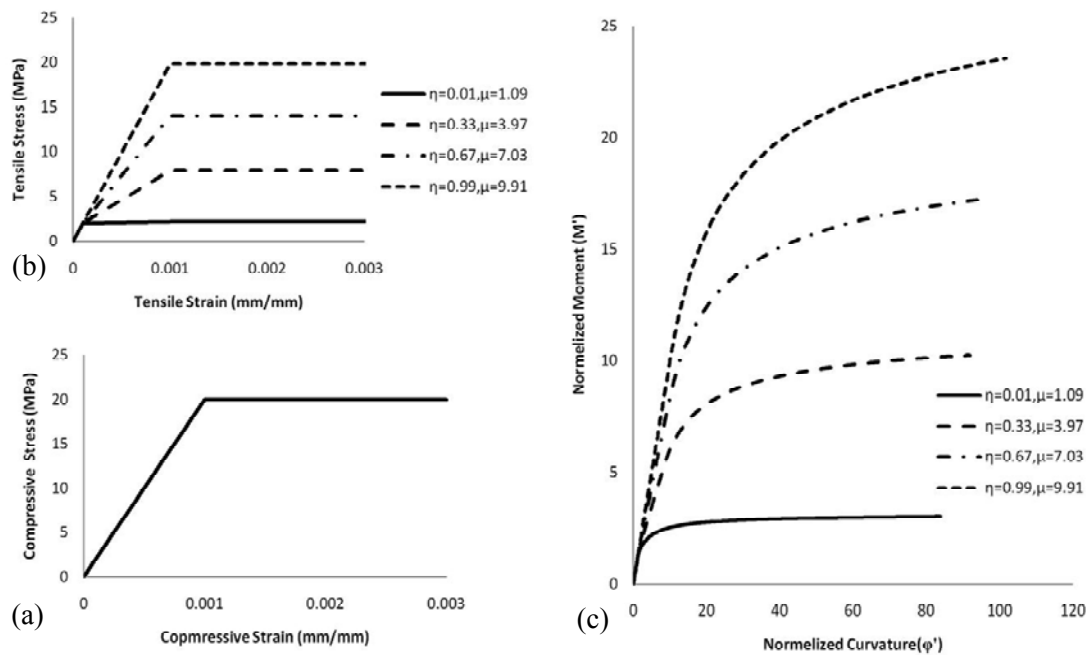

Fig. 14: Parametric study of typical strain hardening material: the effect of parameter γ for $E = 20\ GPa, \varepsilon_{cr} = 0.0001, \alpha = 10, \eta = 0.33, \beta_{tu} = 150,\ \lambda_{cu} = 30$; (a) compresive stress-strain relationship, (b) tensile stress-strain relationship, (c) moment-curvature diagram.
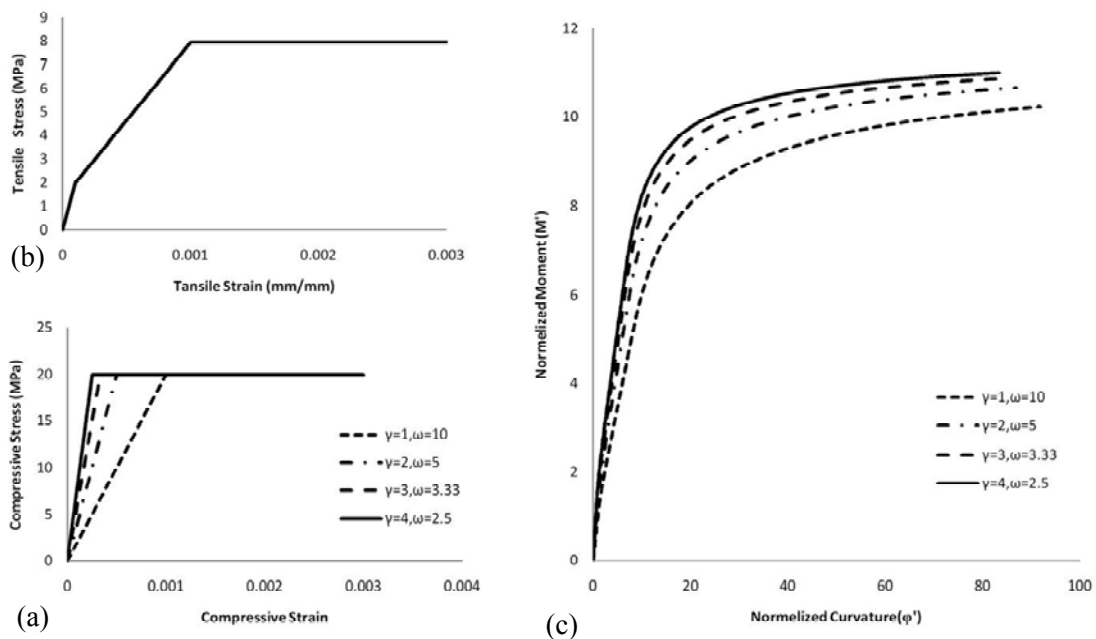
Similar to the strain softening materials, the increase in relative compressive to tensile stiffness at constant compressive to tensile strength ratio $\gamma\omega = 10$ as shown in Fig. 14a and 14b from $0.1 < \frac{\gamma}{\omega} < 1.6$ slightly affect on moment-curvature response. So the transition strain α and the stiffness in the post-cracking tensile range η have a noticable effect on moment-curvature response (Fig. 14c).

8   CONCLUSIONS

Using reinforcement fibers in concrete is an effective method for improving the tensile behavior of concrete. Fiber reinforced concrete (FRC) represents noticeable capacity of bending load bearing and ductility in comparing with plain concrete. To study bending behavior of a bending member made from FRC, the model proposed by Soranakom and Mobasher is selected. Normalized expressions of this model also presented to facilitate calculations. At each of loading step, a trial and error method is used to obtain the correct value of neutral axis depth by equalizing tensile and compression force in the section. Bending moment and curvature are obtained due to the position of neutral axis depth for each stage of loading. The algorithm is terminated when the ultimate tensile strain is governed. To insure the accuracy of algorithm results, an appraisal has been done by using DOCROS software. This evaluation showed that the moment-curvature response estimated from proposed algorithm has a good agreement with ones that obtained from DOCROS software in both strain softening and strain hardening behavior of FRC.

9   ACKNOWLEDGEMENTS

10 REFERENCES

[1] Kang, S.T., Lee, Y., Park, Y.D., and Kim, J.K., (2010), "Tensile fracture properties of an Ultra High Performance Fiber Reinforced Concrete (UHPFRC) with steel fiber", Composite Structures, 92, p. 61-71.

Azurém – 4800-058 Guimarães

[2] ACI 440.2R-08. Guide for the design and construction of externally bonded FRP systems for strengthening concrete structures, Reported by American Concrete Institute, 80 p, July 2008.

[3] Camps, G., Turatsinze, A., Sellier, A., Escadeillas, G., and Bourbon, X., (2008), "Steel-fiber-reinforcement and hydration coupled effects on concrete tensile behavior", Engineering Fracture Mechanics, 75, p. 5207-5216.

[4] V.M.C.F. Cunha, J.A.O. Barros, J.M. Sena-Cruz. "Pullout behaviour of steel fibres in self-compacting concrete", ASCE Journal of Materials in Civil Engineering, 22(1), January 2010.

[5] Soranakom, C., Mobasher, B., (2009), "Flexural design of fiber-reinforced concrete", ACI Materials Journals, p. 461-469.

[6] Soranakom, C., Mobasher, B., (2008), "Correlation of tensile and flexural response of strain softening and strain hardening cement composites", Cement & Concrete Composites, 30, p. 465-477.

[7] Soranakom, C., Mobasher, B., (2007), "Closed form solutions for flexural response o fiber reinforced concrete beams", ASCE Journal of Engineering Mechanics Division (In Press).

[8] Lim, T.Y., Paramasivam, P., and Lee, S.L. (1987), "Analytical model for tensile behavior of steel-fiber concrete", ACI Material Journal, 84(4), p. 286-551.

[9] Salehian, H.R., Barros, J.A.O., Taheri, M., "A design model for strain-softening and strain-hardening fiber reinforced elements failing in bending – implementation and parametric studies", Technical report 24-DEC/E-09, Dep. Civil Eng., School Eng. University of Minho, December 2009.

[10] Ersoy, U., Özcebe, G., (1998), "Moment-curvature relationship of confined concrete sections", Middle East Technical University, Department of Civil Engineering, Ankara, Teknik Dergi, 9(4), p. 1799-1827.

[11] Basto, C.A.A.; Barros, J.A.O., "Numeric simulation of sections submitted to bending", Technical report 08-DEC/E-46, Dep. Civil Eng., School Eng. University of Minho, pp. 73, August 2008.

Annex 1

Calculating the normalized height of compression and tension zones for each stage of normalized tensile strain at bottom fiber (β):

Stage 1 (Fig. 4a)

$$h_{c1} = kd \implies \frac{h_{c1}}{d} = k$$

$$h_{t1} = d - kd = d(1-k) \implies \frac{h_{t1}}{d} = (1-k)$$

Stage 2.1 (Fig. 4b1)

$$h_{c1} = kd \implies \frac{h_{c1}}{d} = k$$

$$\frac{h_{t1}}{d-kd} = \frac{\varepsilon_{cr}}{\beta\varepsilon_{cr}} \implies \frac{h_{t1}}{d(1-k)} = \frac{1}{\beta} \implies \frac{h_{t1}}{d} = \frac{(1-k)}{\beta}$$

$$h_{t2} = d - h_{c1} - h_{t1} \implies \frac{h_{t2}}{d} = \frac{(1-k)(\beta-1)}{\beta}$$

Stage 2.2 (Fig. 4b2)

$$\frac{h_{c1}}{kd} = \frac{\varepsilon_{cy}}{\lambda\varepsilon_{cr}} = \frac{\omega\varepsilon_{cr}}{\frac{k}{1-k}\beta\varepsilon_{cr}} \implies \frac{h_{c1}}{d} = \frac{\omega(1-k)}{\beta}$$

$$h_{c2} = kd - h_{c1} = kd - \frac{\omega(1-k)}{\beta}d \implies \frac{h_{c2}}{d} = \frac{k\beta - \omega(1-k)}{\beta}$$

$$\frac{h_{t1}}{d-kd} = \frac{\varepsilon_{cr}}{\beta\varepsilon_{cr}} \implies \frac{h_{t1}}{d(1-k)} = \frac{1}{\beta} \implies \frac{h_{t1}}{d} = \frac{(1-k)}{\beta}$$

$$h_{t2} = d - h_{c2} - h_{c1} - h_{t1} \implies \frac{h_{t2}}{d} = \frac{(1-k)(\beta-1)}{\beta}$$

Stage 3.1 (Fig. 4c1)

$$h_{c1} = kd \implies \frac{h_{c1}}{d} = k$$

$$\frac{h_{t1}}{d-kd} = \frac{\varepsilon_{cr}}{\beta\varepsilon_{cr}} \implies \frac{h_{t1}}{d(1-k)} = \frac{1}{\beta} \implies \frac{h_{t1}}{d} = \frac{(1-k)}{\beta}$$

$$\frac{h_{t1}}{h_{t1}+h_{t2}} = \frac{\varepsilon_{cr}}{\varepsilon_{trn}} \implies \frac{\varepsilon_{cr}}{\alpha\varepsilon_{cr}} = \frac{\frac{(1-k)}{\beta}d}{\frac{(1-k)}{\beta}d+h_{t2}} \implies \frac{h_{t2}}{d} = \frac{(1-k)(\alpha-1)}{\beta}$$

Azurém – 4800-058 Guimarães

$$h_{t3} = d - kd - h_{t1} - h_{t2} = d - kd - \frac{(1-k)}{\beta}d - \frac{(1-k)(\alpha-1)}{\beta}d \implies \frac{h_{t3}}{d} = \frac{(1-k)(\beta-\alpha)}{\beta}$$

Stage 3.2 *(Fig. 4c2)*

$$\frac{h_{c1}}{kd} = \frac{\varepsilon_{cy}}{\lambda\varepsilon_{cr}} = \frac{\omega\varepsilon_{cr}}{\frac{k}{1-k}\beta\varepsilon_{cr}} \implies \frac{h_{c1}}{d} = \frac{\omega(1-k)}{\beta}$$

$$h_{c2} = kd - h_{c1} = kd - \frac{\omega(1-k)}{\beta}d \implies \frac{h_{c2}}{d} = \frac{k\beta - \omega(1-k)}{\beta}$$

$$\frac{h_{t1}}{d-kd} = \frac{\varepsilon_{cr}}{\beta\varepsilon_{cr}} \implies \frac{h_{t1}}{d(1-k)} = \frac{1}{\beta} \implies \frac{h_{t1}}{d} = \frac{(1-k)}{\beta}$$

$$\frac{h_{t1}}{h_{t1}+h_{t2}} = \frac{\varepsilon_{cr}}{\varepsilon_{trn}} \implies \frac{\varepsilon_{cr}}{\alpha\varepsilon_{cr}} = \frac{\frac{(1-k)}{\beta}d}{\frac{(1-k)}{\beta}d+h_{t2}} \implies \frac{h_{t2}}{d} = \frac{(1-k)(\alpha-1)}{\beta}$$

$$h_{t3} = d - kd - h_{t1} - h_{t2} = d - kd - \frac{(1-k)}{\beta}d - \frac{(1-k)(\alpha-1)}{\beta}d \implies \frac{h_{t3}}{d} = \frac{(1-k)(\beta-\alpha)}{\beta}$$

Annex 2

Calculating the normalized stress at vertices in the stress diagram for each stage of normalized tensile strain at bottom fiber (β):

Stage 1 (Fig. 4a)

$$f_{c1} = \gamma E \lambda \varepsilon_{cr} = \gamma E \left(\frac{k}{1-k}\right) \beta \varepsilon_{cr} \implies \frac{f_{c1}}{E\varepsilon_{cr}} = \frac{\gamma \beta k}{1-k}$$

$$f_{t1} = E \beta \varepsilon_{cr} \implies \frac{f_{t1}}{E\varepsilon_{cr}} = \beta$$

Stage 2.1 (Fig. 4b1)

$$f_{c1} = \gamma E \lambda \varepsilon_{cr} = \gamma E \left(\frac{k}{1-k}\right) \beta \varepsilon_{cr} \implies \frac{f_{c1}}{E\varepsilon_{cr}} = \frac{\gamma \beta k}{1-k}$$

$$f_{t1} = f_{cr} = E \varepsilon_{cr} \implies \frac{f_{t1}}{E\varepsilon_{cr}} = 1$$

$$f_{t2} = E\varepsilon_{cr} + \eta E(\varepsilon_t - \varepsilon_{cr}) = E\varepsilon_{cr} + \eta E(\beta\varepsilon_{cr} - \varepsilon_{cr}) \implies \frac{f_{t2}}{E\varepsilon_{cr}} = 1 + \eta(\beta - 1)$$

Stage 2.2 (Fig. 4b2)

$$f_{c1} = \omega \varepsilon_{cr} \gamma E \implies \frac{f_{c1}}{E\varepsilon_{cr}} = \omega\gamma$$

$$f_{c2} = \omega \varepsilon_{cr} \gamma E \implies \frac{f_{c2}}{E\varepsilon_{cr}} = \omega\gamma$$

$$f_{t1} = f_{cr} = E \varepsilon_{cr} \implies \frac{f_{t1}}{E\varepsilon_{cr}} = 1$$

$$f_{t2} = E\varepsilon_{cr} + \eta E(\varepsilon_t - \varepsilon_{cr}) = E\varepsilon_{cr} + \eta E(\beta\varepsilon_{cr} - \varepsilon_{cr}) \implies \frac{f_{t2}}{E\varepsilon_{cr}} = 1 + \eta(\beta - 1)$$

Stage 3.1 (Fig. 4c1)

$$f_{c1} = \gamma E \lambda \varepsilon_{cr} = \gamma E \left(\frac{k}{1-k}\right) \beta \varepsilon_{cr} \implies \frac{f_{c1}}{E\varepsilon_{cr}} = \frac{\gamma \beta k}{1-k}$$

$$f_{t1} = f_{cr} = E \varepsilon_{cr} \implies \frac{f_{t1}}{E\varepsilon_{cr}} = 1$$

$$f_{t2} = E\varepsilon_{cr} + \eta E(\varepsilon_{trn} - \varepsilon_{cr}) = E\varepsilon_{cr} + \eta E(\alpha\varepsilon_{cr} - \varepsilon_{cr}) \implies \frac{f_{t2}}{E\varepsilon_{cr}} = 1 + \eta(\alpha - 1)$$

Azurém – 4800-058 Guimarães

$$f_{t3} = f_{cst} = \mu E \varepsilon_{cr} \implies \frac{f_{t3}}{E \varepsilon_{cr}} = \mu$$

Stage 3.2 (Fig. 4c2)

$$f_{c1} = \omega \varepsilon_{cr} \gamma E \implies \frac{f_{c1}}{E \varepsilon_{cr}} = \omega \gamma$$

$$f_{c2} = \omega \varepsilon_{cr} \gamma E \implies \frac{f_{c2}}{E \varepsilon_{cr}} = \omega \gamma$$

$$f_{t1} = f_{cr} = E \varepsilon_{cr} \implies \frac{f_{t1}}{E \varepsilon_{cr}} = 1$$

$$f_{t2} = E \varepsilon_{cr} + \eta E (\varepsilon_{trn} - \varepsilon_{cr}) = E \varepsilon_{cr} + \eta E (\alpha \varepsilon_{cr} - \varepsilon_{cr}) \implies \frac{f_{t2}}{E \varepsilon_{cr}} = 1 + \eta (\alpha - 1)$$

$$f_{t3} = f_{cst} = \mu E \varepsilon_{cr} \implies \frac{f_{t3}}{E \varepsilon_{cr}} = \mu$$

Annex 3

Calculating the normalized force component for each stage of normalized tensile strain at bottom fiber (β):

Stage 1 (Fig. 4a)

$$F_{c1} = f_{c1} \times h_{c1} \times \frac{b}{2} = \frac{\gamma\beta k}{1-k} E\varepsilon_{cr} \times kd \times \frac{b}{2} \implies \frac{F_{c1}}{bdE\varepsilon_{cr}} = \frac{\gamma\beta k^2}{2(1-k)}$$

$$F_{t1} = f_{t1} \times h_{t1} \times \frac{b}{2} = \beta E\varepsilon_{cr} \times (1-k)d \times \frac{b}{2} \implies \frac{F_{t1}}{bdE\varepsilon_{cr}} = \frac{\beta(1-k)}{2}$$

Stage 2.1 (Fig. 4b1)

$$F_{c1} = f_{c1} \times h_{c1} \times \frac{b}{2} = \frac{\gamma\beta k}{1-k} E\varepsilon_{cr} \times kd \times \frac{b}{2} \implies \frac{F_{c1}}{bdE\varepsilon_{cr}} = \frac{\gamma\beta k^2}{2(1-k)}$$

$$F_{t1} = f_{t1} \times h_{t1} \times \frac{b}{2} = 1E\varepsilon_{cr} \times \frac{1-k}{\beta}d \times \frac{b}{2} \implies \frac{F_{t1}}{bdE\varepsilon_{cr}} = \frac{1-k}{2\beta}$$

$$F_{t2} = (f_{t1} + f_{t2})h_{t2} \times \frac{b}{2} = \left(1 + 1 + \eta(\beta-1)\right)E\varepsilon_{cr} \times \frac{(1-k)(\beta-1)}{\beta}d \times \frac{b}{2} \implies \frac{F_{t2}}{bdE\varepsilon_{cr}} =$$
$$\frac{(1-k)(\beta-1)(\eta\beta-\eta+2)}{2\beta}$$

Stage 2.2 (Fig. 4b2)

$$F_{c1} = f_{c1} \times h_{c1} \times \frac{b}{2} = \omega\gamma E\varepsilon_{cr} \times \frac{\omega(1-k)}{\beta}d \times \frac{b}{2} \implies \frac{F_{c1}}{bdE\varepsilon_{cr}} = \frac{\omega^2\gamma(1-k)}{2\beta}$$

$$F_{c2} = f_{c2} \times h_{c2} \times b = \omega\gamma E\varepsilon_{cr} \times \frac{k\beta-\omega(1-k)}{\beta}d \times b \implies \frac{F_{c2}}{bdE\varepsilon_{cr}} = \frac{\omega\gamma}{\beta}(\beta k + \omega k - \omega)$$

$$F_{t1} = f_{t1} \times h_{t1} \times \frac{b}{2} = 1E\varepsilon_{cr} \times \frac{1-k}{\beta}d \times \frac{b}{2} \implies \frac{F_{t1}}{bdE\varepsilon_{cr}} = \frac{1-k}{2\beta}$$

$$F_{t2} = (f_{t1} + f_{t2})h_{t2} \times \frac{b}{2} = \left(1 + 1 + \eta(\beta-1)\right)E\varepsilon_{cr} \times \frac{(1-k)(\beta-1)}{\beta}d \times \frac{b}{2}$$

$$\implies \frac{F_{t2}}{bdE\varepsilon_{cr}} = \frac{(1-k)(\beta-1)(\eta\beta-\eta+2)}{2\beta}$$

Stage 3.1 (Fig. 4c1)

$$F_{c1} = f_{c1} \times h_{c1} \times \frac{b}{2} = \frac{\gamma\beta k}{1-k} E\varepsilon_{cr} \times kd \times \frac{b}{2} \implies \frac{F_{c1}}{bdE\varepsilon_{cr}} = \frac{\gamma\beta k^2}{2(1-k)}$$

$$F_{t1} = f_{t1} \times h_{t1} \times \frac{b}{2} = 1E\varepsilon_{cr} \times \frac{1-k}{\beta}d \times \frac{b}{2} \implies \frac{F_{t1}}{bdE\varepsilon_{cr}} = \frac{1-k}{2\beta}$$

$$F_{t2} = (f_{t1} + f_{t2})h_{t2} \times \frac{b}{2} = \big(1 + 1 + \eta(\alpha - 1)\big)E\varepsilon_{cr} \times \frac{(1-k)(\alpha-1)}{\beta}d \times \frac{b}{2} \implies \frac{F_{t2}}{bdE\varepsilon_{cr}} =$$

$$\frac{(1-k)(\alpha-1)(\eta\alpha-\eta+2)}{2\beta}$$

$$F_{t3} = f_{t3} \times h_{t3} \times b = \mu E\varepsilon_{cr} \times \frac{(1-k)(\beta-\alpha)}{\beta}d \times b \implies \frac{F_{t3}}{bdE\varepsilon_{cr}} = \frac{(1-k)(\beta-\alpha)\mu}{\beta}$$

Stage 3.2 (Fig. 4c2)

$$F_{c1} = f_{c1} \times h_{c1} \times \frac{b}{2} = \omega\gamma E\varepsilon_{cr} \times \frac{\omega(1-k)}{\beta}d \times \frac{b}{2} \implies \frac{F_{c1}}{bdE\varepsilon_{cr}} = \frac{\omega^2\gamma(1-k)}{2\beta}$$

$$F_{c2} = f_{c2} \times h_{c2} \times b = \omega\gamma E\varepsilon_{cr} \times \frac{k\beta - \omega(1-k)}{\beta}d \times b \implies \frac{F_{c2}}{bdE\varepsilon_{cr}} = \frac{\omega\gamma}{\beta}(\beta k + \omega k - \omega)$$

$$F_{t1} = f_{t1} \times h_{t1} \times \frac{b}{2} = 1E\varepsilon_{cr} \times \frac{1-k}{\beta}d \times \frac{b}{2} \implies \frac{F_{t1}}{bdE\varepsilon_{cr}} = \frac{1-k}{2\beta}$$

$$F_{t2} = (f_{t1} + f_{t2})h_{t2} \times \frac{b}{2} = \big(1 + 1 + \eta(\alpha - 1)\big)E\varepsilon_{cr} \times \frac{(1-k)(\alpha-1)}{\beta}d \times \frac{b}{2}$$

$$\implies \frac{F_{t2}}{bdE\varepsilon_{cr}} = \frac{(1-k)(\alpha-1)(\eta\alpha-\eta+2)}{2\beta}$$

$$F_{t3} = f_{t3} \times h_{t3} \times b = \mu E\varepsilon_{cr} \times \frac{(1-k)(\beta-\alpha)}{\beta}d \times b \implies \frac{F_{t3}}{bdE\varepsilon_{cr}} = \frac{(1-k)(\beta-\alpha)\mu}{\beta}$$

Azurém – 4800-058 Guimarães

Annex 4

Calculation normalized moment arm of force component for each stage of normalized tensile strain at bottom fiber (β):

Stage 1 (Fig. 4a)

$$y_{c1} = \frac{2}{3}h_{c1} \implies \frac{y_{c1}}{d} = \frac{2}{3}k$$

$$y_{t1} = \frac{2}{3}h_{t1} \implies \frac{y_{t1}}{d} = \frac{2}{3}(1-k)$$

Stage 2.1 (Fig. 4b1)

$$y_{c1} = \frac{2}{3}h_{c1} \implies \frac{y_{c1}}{d} = \frac{2}{3}k$$

$$y_{t1} = \frac{2}{3}h_{t1} \implies \frac{y_{t1}}{d} = \frac{2}{3}\frac{(1-k)}{\beta}$$

$$y_{t2} = y_{t1} + y'_{t2}$$

$$y'_{t2} = \frac{\frac{h_{t2}^2}{6}(f_{t1}-f_{t2})+\frac{h_{t2}^2 f_{t2}}{2}}{\frac{1}{2}(f_{t1}+f_{t2})} \implies \frac{y_{t2}}{d} = \frac{2\eta\beta^2 - \eta\beta - \eta + 3\beta + 3}{3\beta(\eta\beta - \eta + 2)}(1-k)$$

Stage 2.2 (Fig. 4b2)

$$y_{c1} = \frac{2}{3}h_{c1} \implies \frac{y_{c1}}{d} = \frac{2}{3}\frac{\omega(1-k)}{\beta}$$

$$y_{c2} = h_{c1} + \frac{h_{c2}}{2} = \frac{\omega(1-k)}{\beta}d + \frac{k\beta - \omega(1-k)}{2\beta}d \implies \frac{y_{c2}}{d} = \frac{k\beta + \omega(1-k)}{2\beta}$$

$$y_{t1} = \frac{2}{3}h_{t1} = \frac{2}{3}\frac{(1-k)}{\beta}d \implies \frac{y_{t1}}{d} = \frac{2}{3}\frac{(1-k)}{\beta}$$

$$y_{t2} = y_{t1} + y'_{t2}$$

$$y'_{t2} = \frac{\frac{h_{t2}^2}{6}(f_{t1}-f_{t2})+\frac{h_{t2}^2 f_{t2}}{2}}{\frac{1}{2}(f_{t1}+f_{t2})} \implies \frac{y_{t2}}{d} = \frac{2\eta\beta^2 - \eta\beta - \eta + 3\beta + 3}{3\beta(\eta\beta - \eta + 2)}(1-k)$$

Stage 3.1 (Fig. 4c1)

$$y_{c1} = \frac{2}{3}h_{c1} \implies \frac{y_{c1}}{d} = \frac{2}{3}k$$

$$y_{t1} = \frac{2}{3}h_{t1} = \frac{2}{3}\frac{(1-k)}{\beta}d \implies \frac{y_{t1}}{d} = \frac{2}{3}\frac{(1-k)}{\beta}$$

$$y_{t2} = y_{t1} + y'_{t2}$$

$$y'_{t2} = \frac{\frac{h_{t2}^2}{6}(f_{t1}-f_{t2})+\frac{h_{t2}^2 f_{t2}}{2}}{\frac{1}{2}(f_{t1}+f_{t2})} \implies \frac{y_{t2}}{d} = \frac{2\eta\alpha^2-\eta\alpha-\eta+3\alpha+3}{3\beta(\eta\alpha-\eta+2)}(1-k)$$

$$y_{t3} = h_{t1} + h_{t2} + \frac{h_{t3}}{2} \implies \frac{y_{t3}}{d} = \frac{(\alpha+\beta)}{2\beta}(1-k)$$

Stage 3.2 (Fig. 4c2)

$$y_{c1} = \frac{2}{3}h_{c1} \implies \frac{y_{c1}}{d} = \frac{2}{3}\frac{\omega(1-k)}{\beta}$$

$$y_{c2} = h_{c1} + \frac{h_{c2}}{2} = \frac{\omega(1-k)}{\beta}d + \frac{k\beta-\omega(1-k)}{2\beta}d \implies \frac{y_{c2}}{d} = \frac{k\beta+\omega(1-k)}{2\beta}$$

$$y_{t1} = \frac{2}{3}h_{t1} = \frac{2}{3}\frac{(1-k)}{\beta}d \implies \frac{y_{t1}}{d} = \frac{2}{3}\frac{(1-k)}{\beta}$$

$$y_{t2} = y_{t1} + y'_{t2}$$

$$y'_{t2} = \frac{\frac{h_{t2}^2}{6}(f_{t1}-f_{t2})+\frac{h_{t2}^2 f_{t2}}{2}}{\frac{1}{2}(f_{t1}+f_{t2})} \implies \frac{y_{t2}}{d} = \frac{2\eta\alpha^2-\eta\alpha-\eta+3\alpha+3}{3\beta(\eta\alpha-\eta+2)}(1-k)$$

$$y_{t3} = h_{t1} + h_{t2} + \frac{h_{t3}}{2} \implies \frac{y_{t3}}{d} = \frac{(\alpha+\beta)}{2\beta}(1-k)$$

Annex 5

Calculating the neutral axis depth ratio, normalized moment and curvature for each stage of normalized tensile strain at bottom fiber (β):

Stage 1 (Fig. 4a)

$$F_{c1} = F_{t1} \implies \frac{\beta\gamma k^2}{2(1-k)} = \frac{\beta}{2}(1-k) \implies k_1 = \begin{cases} \frac{1}{2} & for\ \gamma = 1 \\ \frac{-1+\sqrt{\gamma}}{-1+\gamma} & for\ \gamma < 1\ or\ \gamma > 1 \end{cases}$$

$$M_1^{'} = F_{c1}y_{c1} + F_{t1}y_{t1} = \frac{\beta\gamma k^2}{2(1-k)}bdE\varepsilon_{cr}\frac{2}{3}kd + \frac{\beta}{2}(1-k)bdE\varepsilon_{cr}\frac{2}{3}(1-k)d$$

$$\implies M_1^{'} = \frac{2\beta[(\gamma-1)k_1^3+3k_1^2-3k_1+1]}{1-k_1}$$

$$\phi_1^{'} = \frac{\frac{\lambda\varepsilon_{cr}}{k_1 d}}{\phi_{cr}} = \frac{\frac{(\frac{k_1\beta}{1-k_1})\varepsilon_{cr}}{k_1 d}}{\phi_{cr}} = \frac{\beta}{2(1-k_1)}$$

Stage 2.1 (Fig. 4b1)

$$F_{c1} = F_{t1} + F_{t2} \implies \frac{\beta\gamma k^2}{2(1-k)} = \frac{(1-k)}{2\beta} + \frac{(1-k)(\beta-1)(\eta\beta-\eta+2)}{2\beta}$$

$$\implies k_{21} = \frac{\beta^2\gamma+\eta(\beta^2-2\beta+1)+2\beta-\beta^2\gamma-1-\sqrt{\gamma^2\beta^4+(\eta(\beta^2-2\beta+1)+2\beta-\beta^2\gamma-1)\gamma\beta^2}}{\eta(\beta^2-2\beta+1)+2\beta-\beta^2\gamma-1}$$

$$D_{21} = \eta(\beta^2-2\beta+1)+2\beta-\beta^2\gamma-1 \implies k_{21} = \frac{\beta^2\gamma+D_{21}-\sqrt{\gamma^2\beta^4+D_{21}\gamma\beta^2}}{D_{21}}$$

$$M_{21}^{'} = F_{c1}y_{c1} + F_{t1}y_{t1} + F_{t2}y_{t2} =$$

$$\frac{\beta\gamma k^2}{2(1-k)}bdE\varepsilon_{cr}\frac{2}{3}kd + \frac{(1-k)}{2\beta}bdE\varepsilon_{cr}\frac{2}{3}\frac{(1-k)}{\beta}d + \frac{(1-k)(\beta-1)(\eta\beta-\eta+2)}{2\beta}bdE\varepsilon_{cr}\frac{2\eta\beta^2-\eta\beta-\eta+3\beta+3}{3\beta(\eta\beta-\eta+2)}(1-k)d =$$

$$\frac{\left[2\beta\gamma+\left(\frac{-2\eta\beta^3+3\eta\beta^2-3\beta^2-\eta+1}{\beta^2}\right)\right]k_{21}^3-3\left(\frac{-2\eta\beta^3+3\eta\beta^2-3\beta^2-\eta+1}{\beta^2}\right)k_{21}^2+3\left(\frac{-2\eta\beta^3+3\eta\beta^2-3\beta^2-\eta+1}{\beta^2}\right)k_{21}-\left(\frac{-2\eta\beta^3+3\eta\beta^2-3\beta^2-\eta+1}{\beta^2}\right)}{1-k_{21}}$$

$$c_{21} = \frac{-2\eta\beta^3+3\eta\beta^2-3\beta^2-\eta+1}{\beta^2} \implies M_{21}^{'} = \frac{(2\beta\gamma+c_{21})k_{21}^3-3c_{21}k_{21}^2+3c_{21}k_{21}-c_{21}}{1-k_{21}}$$

$$\phi_{21}' = \frac{\frac{\lambda \varepsilon_{cr}}{k_{21}d}}{\phi_{cr}} = \frac{\frac{(\frac{k_{21}\beta}{1-k_{21}})\varepsilon_{cr}}{k_{21}d}}{\phi_{cr}} = \frac{\beta}{2(1-k_{21})}$$

Stage 2.2 (Fig. 4b2)

$$F_{c1} + F_{c2} = F_{t1} + F_{t2} \implies \frac{\omega^2 \gamma}{2\beta}(1-k) + \frac{\omega \gamma}{\beta}(\beta k + \omega k - \omega) = \frac{(1-k)}{2\beta} + \frac{(1-k)(\beta-1)(\eta\beta-\eta+2)}{2\beta}$$

$$\implies k_{22} = \frac{\eta(\beta^2 - 2\beta + 1) + 2\beta + \omega^2\gamma - 1}{\eta(\beta^2 - 2\beta + 1) + 2\beta + \omega^2\gamma - 1 + 2\omega\gamma\beta}$$

$$D_{22} = \eta(\beta^2 - 2\beta + 1) + 2\beta + \omega^2\gamma - 1 \implies k_{22} = \frac{D_{22}}{D_{22} + 2\omega\gamma\beta}$$

$$M_{22}' = F_{c1}y_{c1} + F_{c2}y_{c2} + F_{t1}y_{t1} + F_{t2}y_{t2} = \frac{\omega^2\gamma}{2\beta}(1-k)bdE\varepsilon_{cr} \times \frac{2}{3}\frac{\omega(1-k)}{\beta}kd + \frac{\omega\gamma}{\beta}(\beta k + \omega k -$$

$\omega bdE\varepsilon cr \times \beta k + \omega 1 - k2\beta d + 1 - k2\beta bdE\varepsilon cr231 - k\beta d + 1 - k\beta - 1\eta\beta - \eta + 22\beta bdE\varepsilon cr2\eta\beta 2 - \eta\beta - \eta + 3\beta + 33\beta\eta\beta - \eta + 21 - kd = 3\omega\gamma + 2\eta\beta 3 - 3\eta\beta 2 + 3\beta 2 - \omega 3\gamma + \eta - 1\beta 2k222 - 2 \times 2\eta\beta 3 - 3\eta\beta 2 + 3\beta 2 - \omega 3\gamma + \eta - 1\beta 2k22 + 2\eta\beta 3 - 3\eta\beta 2 + 3\beta 2 - \omega 3\gamma + \eta - 1\beta 2$

$$c_{22} = \frac{2\eta\beta^3 - 3\eta\beta^2 + 3\beta^2 - \omega^3\gamma + \eta - 1}{\beta^2} \implies M_{22}' = (3\omega\gamma + c_{22})k_{22}^2 - 2c_{22}k_{22} + c_{22}$$

$$\phi_{22}' = \frac{\frac{\lambda\varepsilon_{cr}}{k_{22}d}}{\phi_{cr}} = \frac{\frac{(\frac{k_{22}\beta}{1-k_{22}})\varepsilon_{cr}}{k_{22}d}}{\phi_{cr}} = \frac{\beta}{2(1-k_{22})}$$

Stage 3.1 (Fig. 4c1)

$$F_{c1} = F_{t1} + F_{t2} + F_{t3} \implies \frac{\beta\gamma k^2}{2(1-k)} = \frac{(1-k)}{2\beta} + \frac{(1-k)(\alpha-1)(\eta\alpha-\eta+2)}{2\beta} + \frac{(1-k)(\beta-\alpha)\mu}{\beta}$$

$$\implies k_{31} = \frac{\eta(\alpha^2 - 2\alpha + 1) + 2\mu(\beta-\alpha) + 2\alpha - 1 - \sqrt{\gamma\beta^2(\eta(\alpha^2 - 2\alpha + 1) + 2\mu(\beta-\alpha) + 2\alpha - 1)}}{\eta(\alpha^2 - 2\alpha + 1) + 2\mu(\beta-\alpha) + 2\alpha - 1 - \beta^2\gamma}$$

$$D_{31} = \eta(\alpha^2 - 2\alpha + 1) + 2\mu(\beta-\alpha) + 2\alpha - 1 \implies k_{31} = \frac{D_{31} - \sqrt{\beta^2\gamma D_{31}}}{D_{31} - \beta^2\gamma}$$

$$M_{31}' = F_{c1}y_{c1} + F_{t1}y_{t1} + F_{t2}y_{t2} + F_{t3}y_{t3} = \frac{\beta\gamma k^2}{2(1-k)}bdE\varepsilon_{cr}\frac{2}{3}kd + \frac{(1-k)}{2\beta}bdE\varepsilon_{cr}\frac{2}{3}\frac{(1-k)}{\beta}d +$$

$$\frac{(1-k)(\alpha-1)(\eta\alpha-\eta+2)}{2\beta}bdE\varepsilon_{cr}\frac{2\eta\alpha^2 - \eta\alpha - \eta + 3\alpha + 3}{3\beta(\eta\alpha-\eta+2)}(1-k)d + \frac{(1-k)(\beta-\alpha)\mu}{\beta}bdE\varepsilon_{cr} \times \frac{(\alpha+\beta)}{2\beta}(1-k)d =$$

$$\left(\frac{1}{k_{31}-1}\right)\left[\left(\frac{3(\mu\beta^2-\mu\alpha^2-\eta\alpha^2+\alpha^2)+2\eta\alpha^3+\eta-1}{\beta^2}-2\beta\gamma\right)k_{31}^3-3\frac{3(\mu\beta^2-\mu\alpha^2-\eta\alpha^2+\alpha^2)+2\eta\alpha^3+\eta-1}{\beta^2}k_{31}^2+\right.$$

$$\left.3\frac{3(\mu\beta^2-\mu\alpha^2-\eta\alpha^2+\alpha^2)+2\eta\alpha^3+\eta-1}{\beta^2}k_{31}-\frac{3(\mu\beta^2-\mu\alpha^2-\eta\alpha^2+\alpha^2)+2\eta\alpha^3+\eta-1}{\beta^2}\right]$$

$$c_{31}=\frac{3(\mu\beta^2-\mu\alpha^2-\eta\alpha^2+\alpha^2)+2\eta\alpha^3+\eta-1}{\beta^2}\implies M_{31}^{'}=\frac{(c_{31}-2\beta\gamma)k_{31}^3-3c_{31}k_{31}^2+3c_{31}k_{31}-c_{31}}{k_{31}-1}$$

$$\phi_{31}^{'}=\frac{\frac{\lambda\varepsilon_{cr}}{k_{31}d}}{\phi_{cr}}=\frac{\frac{(\frac{k_{31}\beta}{1-k_{31}})\varepsilon_{cr}}{k_{31}d}}{\phi_{cr}}=\frac{\beta}{2(1-k_{31})}$$

Stage 3.2 (Fig. 4c2)

$$F_{c1}+F_{c2}=F_{t1}+F_{t2}+F_{t3}\implies\frac{\omega^2\gamma}{2\beta}(1-k)+\frac{\omega\gamma}{\beta}(\beta k+\omega k-\omega)=\frac{(1-k)}{2\beta}+\frac{(1-k)(\alpha-1)(\eta\alpha-\eta+2)}{2\beta}+$$

$$\frac{(1-k)(\beta-\alpha)\mu}{\beta}\implies k_{32}=\frac{\omega^2\gamma+\eta\alpha^2+2(\mu\beta-\eta\alpha-\mu\alpha+\alpha)+\eta-1}{\omega^2\gamma+\eta\alpha^2+2(\mu\beta-\eta\alpha-\mu\alpha+\alpha)+\eta-1+2\omega\gamma\beta}$$

$$D_{32}=\omega^2\gamma+\eta\alpha^2+2(\mu\beta-\eta\alpha-\mu\alpha+\alpha)+\eta-1\implies k_{32}=\frac{D_{32}}{D_{32}+2\omega\gamma\beta}$$

$$M_{32}^{'}=F_{c1}y_{c1}+F_{c2}y_{c2}+F_{t1}y_{t1}+F_{t2}y_{t2}+F_{t3}y_{t3}$$

$$=\frac{\omega^2\gamma}{2\beta}(1-k)bdE\varepsilon_{cr}\times\frac{2}{3}\frac{\omega(1-k)}{\beta}kd+\frac{\omega\gamma}{\beta}(\beta k+\omega k-\omega)bdE\varepsilon_{cr}\times\frac{\beta k+\omega(1-k)}{2\beta}d+$$

$$\frac{(1-k)}{2\beta}bdE\varepsilon_{cr}\frac{2}{3}\frac{(1-k)}{\beta}d+\frac{(1-k)(\alpha-1)(\eta\alpha-\eta+2)}{2\beta}bdE\varepsilon_{cr}\frac{2\eta\alpha^2-\eta\alpha-\eta+3\alpha+3}{3\beta(\eta\alpha-\eta+2)}(1-k)d+\frac{(1-k)(\beta-\alpha)\mu}{\beta}bdE\varepsilon_{cr}\times$$

$$\frac{(\alpha+\beta)}{2\beta}(1-k)d$$

$$=(\frac{3(\mu\beta^2-\mu\alpha^2-\eta\alpha^2+\alpha^2)+2\eta\alpha^3-\omega^3\gamma+\eta-1}{\beta^2}+3\omega\gamma)k_{32}^2-2\frac{3(\mu\beta^2-\mu\alpha^2-\eta\alpha^2+\alpha^2)+2\eta\alpha^3-\omega^3\gamma+\eta-1}{\beta^2}k_{32}+$$

$$\frac{3(\mu\beta^2-\mu\alpha^2-\eta\alpha^2+\alpha^2)+2\eta\alpha^3-\omega^3\gamma+\eta-1}{\beta^2}$$

$$c_{32}=\frac{3(\mu\beta^2-\mu\alpha^2-\eta\alpha^2+\alpha^2)+2\eta\alpha^3-\omega^3\gamma+\eta-1}{\beta^2}\implies M_{31}^{'}=(c_{32}+3\omega\gamma)k_{32}^2-2c_{32}k_{32}+c_{32}$$

$$\phi_{32}^{'}=\frac{\frac{\lambda\varepsilon_{cr}}{k_{32}d}}{\phi_{cr}}=\frac{\frac{(\frac{k_{32}\beta}{1-k_{32}})\varepsilon_{cr}}{k_{32}d}}{\phi_{cr}}=\frac{\beta}{2(1-k_{32})}$$